IEEE Access
Multidisciplinary | Rapid Review | Open Access Journal

Received 29 March 2023, accepted 10 April 2023, date of publication 13 April 2023, date of current version 20 April 2023.

Digital Object Identifier 10.1109/ACCESS.2023.3266820

RESEARCH ARTICLE

A Comprehensive Analysis, Design, and Experimental Evaluation of Single-Loop Polygonal Slotted RF Resonators and WPT Systems

KASSEN DAUTOV, GALYMZHAN NAURYZBAYEV, (Senior Member, IEEE), AND MOHAMMAD HASHMI, (Senior Member, IEEE)
School of Engineering and Digital Sciences, Nazarbayev University, Astana 010000, Kazakhstan

Corresponding author: Mohammad Hashmi (mohammad.hashmi@nu.edu.kz)

This work was supported in part by Nazarbayev University under Grant 021220CRP0222, Grant 11022021CRP1513, and Grant 20122022FD4113.

ABSTRACT A thorough analysis of slotted ground plane (SGP)-based resonators designed for wireless power transfer (WPT) applications is reported in this paper. For the first time, some new findings that relate a resonator and WPT performance metrics to the slot shape, quality factor (Q), and radiation loss are presented in a very comprehensive manner. As a case study, a single-loop polygonal shape was considered to carry out all analyses and investigations. It has been identified that the slot shape has no impact on the performance of resonators and, hence, developed WPT. Instead, the performance is hugely dependent on Q of resonators regulated by the chosen slot area. These findings allow the conceptualization of systematic analysis of WPT systems and the development of design schemes that are readily realizable, and they also enable significant improvement in power transfer efficiency (PTE). The developed prototypes conforming to the industrial, scientific, and medical frequency bands show an enhancement in PTE to the extent of 11% during the measurements. The proposed analysis and design approach are very important steps in advancing state-of-the-art radio-frequency WPTs. In essence, this has the potential to reinvigorate the stagnated SGP-based WPT systems so as to facilitate the requirements of low-power applications.

INDEX TERMS Magnetic resonant coupling (MRC), quality factor (Q), radiation loss (RL), resonator, slotted ground plane (SGP), wireless power transfer (WPT).

I. INTRODUCTION

Wireless power transfer (WPT) systems have the potential to bring a complete turnaround in a variety of emerging applications. They have been lately employed in a number of segments such as biomedicine, consumer electronics, micro-robotics, vehicular, and emerging wireless technologies and can be broadly classified into far- and near-field types [1], [2], [3]. If the former is accomplished using protocols, namely, time-switching and power-splitting relaying techniques, the latter is achieved by following any of the coupling-based techniques (*i.e.*, capacitive or inductive) [4]. As a concept, magnetic resonant coupling (MRC) also falls under the umbrella of inductive coupling. This enables the synchronization of the resonance of the transmitter (Tx) and receiver (Rx) to enhance the WPT performance [5]. In this instance, it should be noted that a number of factors, namely, power level, coupling degree, operating frequency, resonator structure, and size, influence the performance of MRC-based WPTs [6]. Tx and Rx in such WPTs are essentially resonators for which a number of design techniques exist in literature. For example, cubic high dielectric and cavity resonators have proven their usefulness in the highly efficient WPT design [7]. Nonlinear resonators, on the other hand, are

The associate editor coordinating the review of this manuscript and approving it for publication was Diego Masotti.

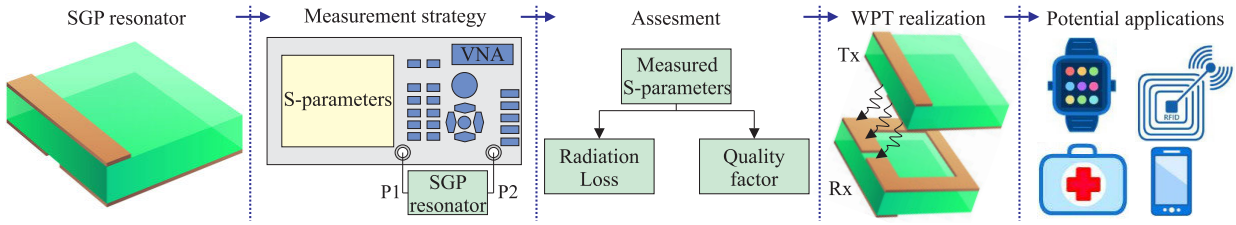

FIGURE 1. The conceptual depiction: SGP resonator evualuation strategy and WPT development.

extremely effective at solving the WPT constraints caused by coupling variations [8]. The coils with a parallel configuration, as compared to the series ones, are more suitable for obtaining the load-independent WPTs [9].

To cater to the requirements of low-power applications, the use of slotted ground plane (SGP)-based resonators has recently piqued interest [10], [11], [12], [13], [14], [15]. It should be noted that this technique is also known as the defected ground structure. The SGP method brings a number of benefits including circuit size reduction, quality factor (Q) enhancement, design simplicity, and low losses [16]. The literature is replete with reports that discuss methodologies for resolving the WPT challenges by utilizing distinct slots such as ellipse, square, triangle, circle, hexagon, U, C, E, H, *etc.* [17], [18], [19]. Furthermore, the high Q resonators (in any form) increase the energy coupling, which successfully compensates for the efficiency degradation caused by low couplings [6]. Interestingly, SGP-shapes demonstrate their effectiveness in obtaining high Q [20]. As a result, there are some reports that made utilization of the high Q resonators to develop the SGP-type WPT with excellent performances [19]. In addition, radiation loss (RL) also adversely affects various performance metrics of WPTs. It has been shown that the SGP approach has the potential to significantly reduce RL over a wide spectrum of frequency bands and is, thus, considered an excellent candidate for the design of WPTs [21], [22].

A literature survey reveals that the development of SGP-based WPT systems entails the use of a slot shape in the ground plane to optimize their performances [19]. This leads to the premise that selecting a slot type is commonly a dilemma. However, these papers often overlook the other critical parameters such as the slow wave factor (SWF), generated magnetic (H) field, Q, and RL that are equally critical in the design of WPT systems. In this regard, it is imperative to note that the present authors analyzed the SGP-type resonators for achievable SWF and H-field [23]. Therefore, for the sake of complete SGP-based resonator analysis, this particular work aims to conceptualize various SGP-based WPT architectures in terms of two other parameters. In turn, this aids in the development of a mechanism for the identification of the slot shape that can provide superior performance. Consequently, it can be assumed that the explorations and outcomes of this work aid in the development of high-performance SGP-based WPT systems extremely useful for several application fields.

TABLE 1. Application areas of SGP-based near-field WPT.

Ref.	Size (mm×mm)	PTD (mm)	Applications
[10]	30 × 15	15	Biomedical Implants
[11]	20 × 20	10	Biomedical Implants
[12]	43 × 38	23	RFIDs / Smart Cards / Sensors
[13]	20 × 20	10	Portable Devices
[14]	25 × 25	10	Sensor Networks / RFIDs
[17]	18 × 18	11	Biomedical Implants
[18]	15 × 10	3.5	Electronic Devices

Recently, the near-field SGP-based WPT systems have found usefulness in a wide range of applications [13], [14]. In this regard, it is worth noting that biomedicine is found to be an emerging application area for WPT in particular [2], [15]. Because of its human safety, short power transfer distance, and excellent performance, near-field WPT has been particularly well-suited to power numerous implanted medical devices such as brain stimulators, intraocular implants, cardiac pressure sensors, pacemakers, and capsule endoscopes [4]. On the other hand, they also find effectiveness in numerous applications including but not limited to consumer electronics, micro-robotics, RFIDs, and low-power sensors [10], [11], [12], [13], [14], [17], [18]. For the sake of completeness, Table 1 summarizes the application areas of near-field SGP-type WPT systems.

In principle, SGP-based resonator evaluation is complex and necessitates an extremely accurate methodology. The specific resonator assessment strategy applied in this work is illustrated in Fig. 1. It is pertinent to note that the SGP-type resonator exhibits a two-port network property, therefore, can be characterized through the measured scattering (S) parameters obtained using a vector network analyzer (VNA). As a consequence, the S-parameters allow for the analysis of two critical parameters such as RL and Q. In this paper, as a case study, generic single-loop polygonal slots in the ground plane are considered to investigate their effect on the performance of the resonator and resultant WPT system. As a result, the thorough analysis and subsequent findings of this work have led to the below-listed contributions:

- The development of a theoretical postulation that resonators with a wide variety of slot shapes and slot areas exhibit excellent RL at the frequency range below 1 GHz and the subsequent experimental demonstration.
- The investigation and analysis show that the single-loop polygonal slots with different numbers of sides and

possessing the same slot areas exhibit nearly the same achievable Q.
- The experimental evaluation of the developed theoretical postulations about the impact of slot shapes and slot areas on the performance of the resonators and the eventual WPT systems. In particular, demonstration of the use of smaller slots (*i.e.*, greater Q) for achieving higher power transfer efficiency (PTE). The exampling prototype achieved enhancement of 11% in PTE with the reduction in the slot area.

Section II provides an overview of resonators associated with the traditional and the SGP technique. Section III examines and experimentally evaluates various single-loop polygonal slot-based resonators in terms of their achievable Q and RL. Furthermore, the WPT system development, as well as their experimental validation and performance evaluation, are discussed in Section IV. Finally, Section V summarizes the analysis and explorations of this work.

II. RESONATOR OVERVIEW

It is well established that the characteristics of resonators regulate the performance of eventual WPT systems. Therefore, a brief discussion and explanation of the conventional and the SGP-based resonator design strategies are included in this section to understand the nuances involved in the designs.

A. CONVENTIONAL APPROACH

The MRC technique allows high PTE over relatively close proximity by means of proper resonance matching between `Tx` and `Rx` coils. Thus, conventional coils, including planarized ones, have been broadly utilized to develop WPT end-modules (*i.e.*, resonators). Near the resonance, they can be modeled as parallel resistance, inductance, and capacitance (*RLC*) circuits. The depiction of the conventional coil and its equivalent circuit is given in Fig. 2. In these structures, a proper *LC* combination generates the angular resonant frequency (ω_0) given by (1) [24]. Here, f_0 represents the resonant frequency. On the other hand, the input impedance of the parallel *RLC* circuit is calculated using (2) [25].

$$\omega_0 = 2\pi f_0 = \frac{1}{\sqrt{LC}}, \tag{1}$$

$$Z_{in} = \left(\frac{1}{R} + \frac{1}{j\omega L} + j\omega C\right)^{-1}. \tag{2}$$

In this instance, it should be noted that precise modeling depends on the techniques employed to design resonators. For instance, a current source is utilized to analyze the parallel *RLC* circuits. In such a scenario, the source's impedance is considered to be completely resistive at the resonant frequency. Furthermore, an open circuit is formed by a parallel combination of L and C. As a result, the total current passes through the resistor at the resonance. Finally, based on the current divider rule and the current flowing through the resistor, as a function of frequency, (3) is obtained [25]. Here, I_S is a current provided by the source.

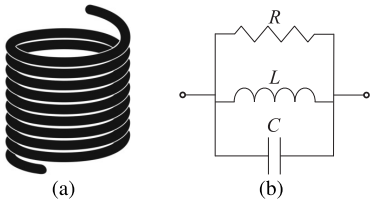

FIGURE 2. A conventional resonator structure: (a) coil; (b) parallel *RLC* equivalent circuit.

$$I_R = I_S \frac{j\omega L}{(R - \omega^2 LCR) + j\omega L}. \tag{3}$$

B. SGP TECHNIQUE

In general, the last decade has seen an increased interest in the SGP-based design of high-frequency circuits [16]. It provides a number of benefits including circuit miniaturization [19]. Furthermore, variously shaped SGPs are employed to improve the performance of microstrip technology-based circuits. For example, the use of SGPs can assist in realizing the enhanced polarization purity, increased bandwidth at *X/Ku*-bands, and filtering structures with different characteristics [26], [27]. The key premise behind the SGP methodology is to create slots on the ground plane in order to change a current flow path [28]. The influence of etched slots is multifaceted and, as a result, they can lead to a variety of outcomes. In essence, in the presence of slots in the ground plane a typical behavior of transmission lines is significantly modified [5]. As a consequence, microstrip lines (MLs) demonstrate different stop-band features. Additionally, the characteristic impedance of the SGP circuit can be found using (4) where $Z_0 = 50\ \Omega$. Furthermore, Γ is computed as $|\Gamma| = 10^{\frac{S_{11}}{20}}$, where S_{11} in dB [29].

$$Z_{SGP} = Z_0 \sqrt{\frac{1 + |\Gamma|}{1 - |\Gamma|}}. \tag{4}$$

Generally, either the parallel *RLC* or *LC* can be used to model the unloaded SGP-based resonator which has the quasi-lumped resonant circuit behavior [30]. The respective values of C, L, and R can be extracted from available electromagnetic (EM) simulation software and in consonance with (5)−(7) [23]. Here, the term f_0 represents the resonance and f_c stands for the "−3" dB cut-off frequencies.

$$C = \frac{f_c}{4\pi Z_0 (f_0{}^2 - f_c{}^2)}, \tag{5}$$

$$L = \frac{1}{4\pi^2 f_0^2 C}, \tag{6}$$

$$R = \frac{2Z_0}{\sqrt{\frac{1}{|S_{11}(2\pi f_0)|^2} - \left(2Z_0\left(2\pi f_0 C - \frac{1}{2\pi f_0 L}\right)\right)^2} - 1}. \tag{7}$$

It is also pertinent to mention that the units for C, L, and R are pF, nH, and kΩ, respectively. In addition, unloaded Q of

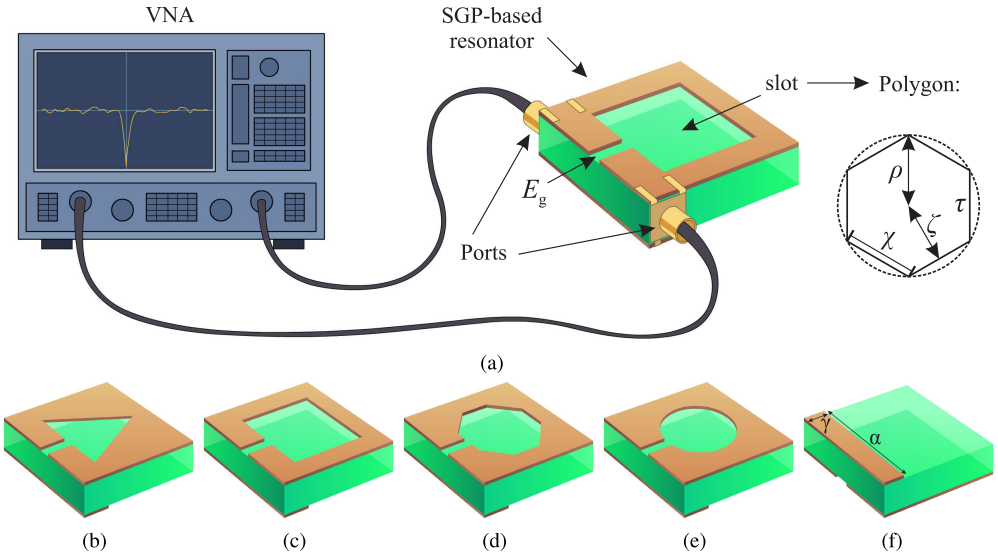

FIGURE 3. The structure of SGP-based resonators (bottom/top view) and their measurement: (a) characterization setup; (b) $\tau = 3$; (c) $\tau = 4$; (d) $\tau = 8$; (e) $\tau = 32$; (f) top-side.

the parallel resonant circuit can be expressed by (8) [20].

$$Q = 2\pi f_0 CR. \tag{8}$$

III. PERFORMANCE EVALUATION

The properly designed SGP-based resonator architectures are critical components of magnetically coupled WPTs. It should be noted that these designed resonators predetermine the eventual WPT performance. Hence, there is a need for a thorough analysis of resonators that can be regarded as the first vital step toward a successful WPT system. Fig. 3 illustrates the SGP-type resonator, its typical measurement, and characterization setup. Its structure consists of three layers, *i.e.*, a single layer of a dielectric material, and two layers of copper. The slots are introduced on the bottom-side (*i.e.*, ground plane) while the top-side stays unchanged. The excitation gap (E_g) placed below ML aids in the creation of a resonance. It is worth noting that the analysis, design, and optimizations in this work are carried out using EM and circuit simulation software such as *CST Studio Suite* and *Keysight ADS*, respectively. The required EM simulations were performed in compliance with the commonly adopted simulation strategy. Particularly, the RO4350B substrate and copper (annealed) were acquired from the available material library whereas the incorporated capacitors were added as lumped elements. The excitation of SGP-based resonators was accomplished using discrete ports. In addition, all EM simulations were carried out with open boundary conditions in all directions employing the `hexahedral` mesh.

The *polygonal single-loop slots*, shown in Fig. 3b, are studied in this work. By its feature polygons are closed geometrical figures confined by straight sides. Besides that, the slots under consideration are assumed to be universal as they can change the geometry in accordance with the modification in the number of sides (τ). For example, the slot

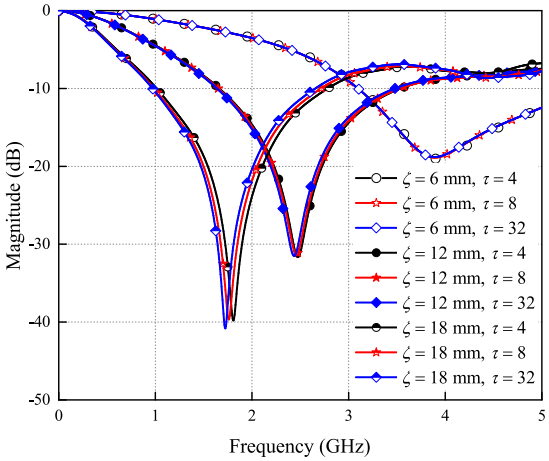

FIGURE 4. Obtained S_{21} of SGP-resonators.

can be a triangle, square, octagon, hexagon, or circle when the sides of a polygon are altered. As a consequence, this allows simultaneous observation of the impact of multiple slots on resonator key parameters. Moreover, it is apparent that a large value of τ leads to a circular shape. In these explorations, however, $\tau = 32$ is sufficient to form a circle considering the small area of developed resonators. In addition, the important parameters of the studied slot shapes such as the in-radius (ζ) and length of sides (χ) can be defined using (9) and (10), respectively. Here, $\tau \in 3, 4, \ldots 32$ and, apparently, $\uparrow \tau \rightarrow \downarrow \chi$.

$$\zeta = \rho \cos \frac{180^\circ}{\tau}, \tag{9}$$

$$\chi = 2\rho \sin \frac{180^\circ}{\tau}. \tag{10}$$

All SGP-based resonators in this work possess the same circuit area (25×25 mm^2) which allows for impartial analysis

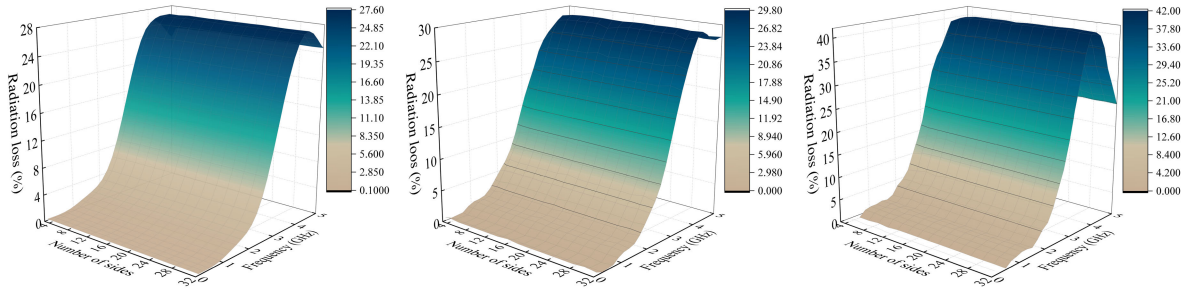

FIGURE 5. Simulated RL: (a) $\zeta = 6$ mm; (b) $\zeta = 12$ mm; (c) $\zeta = 18$ mm.

and evaluations. The selected substrate is Rogers' RO4350B with a permittivity of 3.48 and height (h_s) of 1.524 mm. Furthermore, the substrate is coated, from both sides, by copper which has a thickness (h_c) of 0.035 mm. Besides, P1 and P2 (input and output ports) of resonators are connected using ML with the 3.4 mm width (γ). In turn, the ports facilitate the connection of resonators to VNA for characterization purposes. It is pertinent to note that polygonal shapes with different ζ were considered during the studies for the sake of accuracy and scalability. Particularly, chosen ζ of 6 mm, 12 mm, and 18 mm resulted in different areas. Besides, τ was changed from 3 to 32 to form different slots which, in turn, led to various current flow paths on the ground plane. Analyses were performed in terms of two main resonator parameters such as the *radiation loss and quality factor*. The subsequent discoveries of analyses and their experimental validation are discussed in the remaining parts of this section.

At the outset, the effect of slot type and area variations on the resonant frequency is presented in Fig. 4. It can be observed that the enlargement in the slot area leads to the resonance shift to lower frequency bands. It is apparent that almost the same resonances occurred when τ was changed. Furthermore, it is important to note that τ has a greater influence on the considered polygonal shape for slots with bigger areas. As a result, there is a minor difference in the resonances for resonators with $\zeta = 18$ mm.

A. RADIATION LOSS

In this work, studied RL effectively includes the radiation and scattering effect of SGP-type resonators. The extensive explorations of RL within the realm of microwave and wireless components are of great interest. The SGPs' EM fields (*i.e.*, electric and magnetic) are distributed in an open space, which can result in significant EM radiation. Furthermore, this phenomenon may lead to an increase in insertion loss [31]. Therefore, during the design of the microwave components, the predominant aim is to reduce the RL level [21]. In addition, RL of the developed SGP-type resonators can be computed using (11) [22].

$$\Upsilon = 1 - \left(|S_{11}|^2 + |S_{21}|^2\right). \tag{11}$$

The RL dependence on τ of polygonal single-loop-based resonators obtained from the EM simulation environment is shown in Fig. 5. These results reveal that RL possesses smaller values at lower frequencies as compared to higher bands. Although RL does not exceed 40% in any of the studied cases, the resonators with smaller slots demonstrate lower values. This observation implies that the circuit resistance rises with higher ζ (*i.e.*, less metal on the ground plane) therefore RL also increases. In particular, regardless of the shape and ζ variations, RL is less than 5% for the frequency range up to 1 GHz. Therefore, it is safe to state that *the number of sides has no impact on RL of resonators with the considered shape and slot area* for frequencies below 1 GHz.

B. QUALITY FACTOR

Q of resonant structures can be defined from two aspects: stored energy and bandwidth. In essence, the former is the ratio of the stored energy to lost power at the resonant frequency, whereas the latter is related to the sharpness of the occurred resonance [32], which is considered in this work. It is important to mention that high-performance coupling-based WPTs rely on high Q resonators. For example, as the transmission distance between Tx and Rx increases, the coupling weakens, necessitating a rise in Q of resonators in order to improve PTE [33]. Keeping this in perspective, a number of reports discussed the improvement in Q by changing the coil structures or proposing new innovative solutions [34]. Furthermore, the SGP method can also enable achieving high Q by controlling the geometry of given SGP shapes [19]. In this work, Q was defined following the conventional method which uses (12), where β represents the "-3" dB bandwidth of S_{21} [35]. The *RLC* or *LC* equivalent circuits can be used to obtain the required S_{21} parameters and subsequently determine Q [20]. It should be noted that both approaches can be employed in the Q calculation.

$$Q = \frac{f_0}{\beta}. \tag{12}$$

The SGP-type resonator exhibits resonance phenomena, with L produced by ground whilst E_g provides constant capacitance. It is apparent that it results in a resonating frequency that potentially may vary from the desired one. Consequently, there is a need for a solution that helps control the resonance (*i.e.*, the system's operating frequency). Within the concept of SGP-based resonators, it can be achieved by

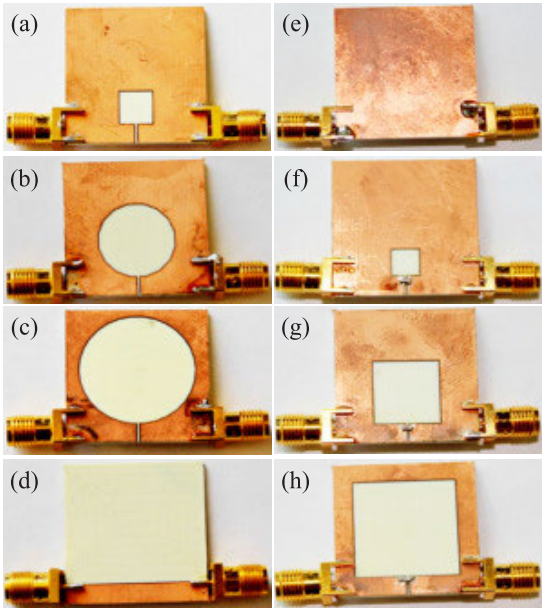

FIGURE 6. Fabricated resonators: (a) $\zeta = 6$ mm, $\tau = 4$; (b) $\zeta = 12$ mm, $\tau = 16$; (c) $\zeta = 18$ mm, $\tau = 32$; (d) top-side; (e) no slot; (f)–(h) resonators with loaded SMD capacitors.

loading a capacitor (C_e) to E_g. Subsequently, C_e with an aptly value aid in the control of resonant frequency. In this work, appropriate values of C_e were incorporated to further investigate the chosen slot shapes and achievable Q at the practical frequencies. It is pertinent to note that various frequency bands are employed within the regime of wireless communications. In order to provide practical viability to the investigated SGP-based resonators, and subsequent WPT, the operating frequency must comply with the well-accepted standards [1]. Therefore, in this work, the selected frequency was the practical ISM (industrial, scientific, and medical) band of 900 MHz. Furthermore, τ of the polygonal shape was fixed to 4 (which is common for all) and only ζ was modified.

C. WPT PERFORMANCE EVALUATION

In general, the main performance metrics for near-field WPTs are considered the size of the coupled resonators, power transfer distance (PTD), and PTE [19]. It is apparent that the mentioned key characteristics unambiguously define the efficacy of developed WPT for any potential application. However, it is worthwile to note that some applications may demand the superiority of a particular metric. For example, the size of resonators is more important for biomedical applications whereas consumer electronics may require WPT with high PTE. It is pertinent to highlight that SGP-based WPT is still in its early development stage, and hence no widely accepted standard performance indicators exist. Therefore, there have been efforts to benchmark WPT by proposing a standard and optimal metric capable of incorporating all three above-mentioned key parameters. Consequently, the metric known as the figure of merit (FoM), defined as $FoM = \frac{PTE \times PTD}{\sqrt{resonator\ area}}$, has been proposed and extensively used to assess the WPT effectiveness [10], [11], [12], [13], [14].

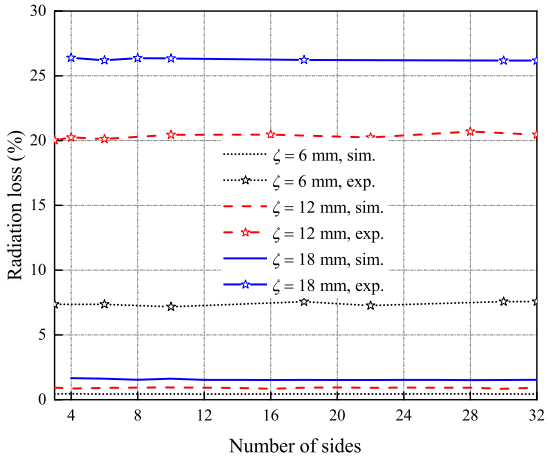

FIGURE 7. Experimental RL vs τ.

D. EXPERIMENTAL VALIDATION OF RESONATORS

The prototypes depicted in Fig. 6, included for investigation purposes, were fabricated using the same substrate (*i.e.*, Rogers' RO4350B) as utilized during the EM simulations. Furthermore, the experimental evaluations of these prototypes were carried out using the Keysight PNA-X (N5247B)-based setup shown in Fig. 6.

Fig. 7 compares the simulation and experimental of the RL results for resonators with different slots. It is worth noting that the experimental RL was calculated using the measured S_{21} and (11). Apparently, the obtained experimental results are in perfect consonance with the corresponding simulations. There is an anomaly and it's evident with a minor effect of τ on RL. However, the resonators with greater ζ exhibit a trend of having higher RL. It is imperative to note that during the EM simulations circuit is considered ideal hence it is a common practice to have a disagreement between the simulation and measured results [17], [36]. This discrepancy may also occur due to the prototyping precision, tolerance of used components, and additional losses associated with the employed adapters and semi-rigid cables during experiments. Experimental RL of about 7.5%, 20.5%, and 26% were computed for the SGP-based resonators with ζ of 6 mm, 12 mm, and 18 mm, respectively. It is worth mentioning that these values were calculated considering the initial resonance of SGP-based resonators.

For the evaluation of Q, one can assess the obtained Q for polygonal single-loop SGP-based resonators with different τ shown in Fig. 8. It is apparent that although τ of the proposed slot is shape-dependent all resonators achieve nearly same Q. However, it further reveals that the resonators with smaller slots possess higher Q. This finding leads to the idea that Q is more reliant on the slot area rather than the type of shapes. As a consequence, it is fair to conclude that *the shape does not play a significant role in achieving high Q*. Furthermore, the obtained experimental results in Fig. 8 also validate this discovery. The measured Q values of the resonators with $\zeta = 18$ mm slot are almost three times smaller than the ones

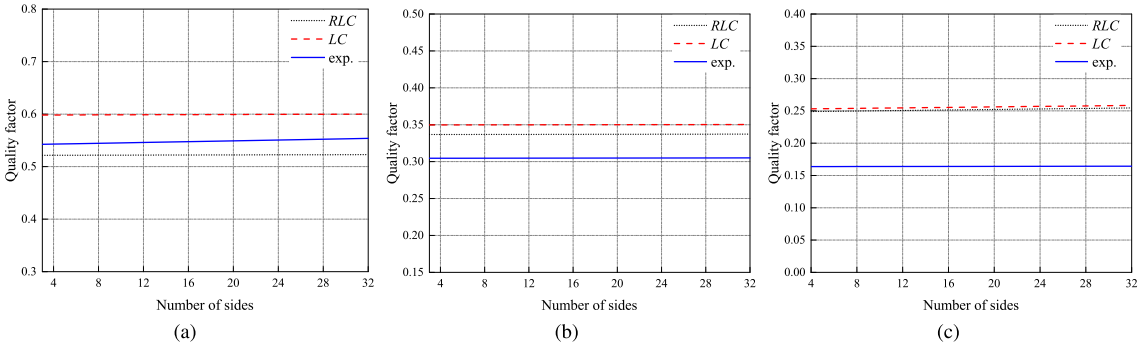

FIGURE 8. Q vs polygonal slots with different τ: (a) $\zeta = 6$ mm; (a) $\zeta = 12$ mm; (a) $\zeta = 18$ mm.

TABLE 2. Lumped element values corresponding to the resonance at 900 MHz.

SGP resonator	R (kΩ)	L (nH)	C_e (pF)	$C_{Tot.} = C_e + E_g$ (pF)
$\tau = 4,\ \zeta = 6$ mm	8.03	5.3	3.9	5.89
$\tau = 4,\ \zeta = 12$ mm	17.76	17.21	1.3	1.82
$\tau = 4,\ \zeta = 18$ mm	23.71	34.94	0.6	0.89

with $\zeta = 6$ mm slot. In addition, it can be easily gleaned that experimental Q of the resonators with the smallest slots falls between computed Q using the *RLC* and *LC* methods. However, for bigger slots, the experimental Q values are smaller as compared to the EM simulated results. This slight anomaly may be due to the greater losses related to larger slots. Thus, it is safe to convey that both approaches can be only used to approximate realized Q.

On the other hand, Fig. 9 presents the EM and circuit simulations along with the experimental results of the SGP-based resonators. It can be clearly seen that the resonance for all three cases occurs at 900 MHz. It can also be seen that the resonator with a smaller slot area possesses higher Q and it reiterates the earlier findings mentioned above. In particular, using (12) gives the respective Q of 3.72, 1.22, and 0.67 for $\zeta = 6$ mm, $\zeta = 12$ mm, and $\zeta = 18$ mm. Additionally, Table 2 presents the respective values of loaded capacitors (C_e), L, and, R corresponding to the resonance at 900 MHz.

IV. WPT DEVELOPMENT

The use of the MRC-based technique in the design of near-field WPT systems significantly enhances the overall system performance. Apparently, the successful realization of this method highly depends on the performance of SGP-based resonators which act as the system's end modules. In such systems, one resonator acts as Tx whereas another one is Rx [5]. Essentially, the optimized resonators, meeting the WPT specification requirements, can be coupled at a certain proximity to achieve the power transfer wirelessly. In this instance, it is important to highlight that the coupled resonators must oscillate at an identical frequency. The creation of an EM field is successfully achieved when the appropriate coupling is met. It has been well established that PTE of coupling technique-based WPT systems is mainly influenced by two key factors, namely, the coupling coefficient (k) and

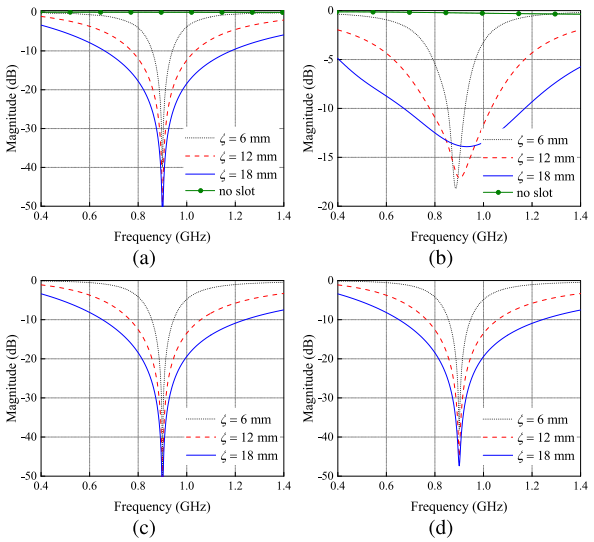

FIGURE 9. $|S_{21}|$ vs frequency results for resonators with $\tau = 4$ and different ζ: (a) sim.; (b) exp.; (c) *LC*; (d) *RLC*.

Q of unloaded resonators [33]. It has been reported that k decreases rapidly with the increase in a separation distance between the coupled resonators and this, in turn, leads to reduced PTE [6]. Therefore, the high Q resonators are used to achieve high PTE from WPT systems with weak k [37].

The coupling phenomenon is divided into three main types: i) undercoupling – the range where resonators are poorly coupled and, as a result, PTE drops abruptly; ii) overcoupling – occurs when two resonators are placed at very close proximity. It leads to the splitting of the resonant frequency and, subsequently, the highest efficiency is obtained at frequencies other than the initially designed working frequency; iii) critical coupling – this point is considered to be optimal as the maximum energy transfer, between Tx and Rx, is achieved [8]. For the ideal WPT, k and Q define the maximum achievable efficiency which can be calculated using (13) [33].

$$PTE_{max} = \frac{k^2 Q_{\mathrm{Tx}} Q_{\mathrm{Rx}}}{\left(1 + \sqrt{1 + k^2 Q_{\mathrm{Tx}} Q_{\mathrm{Rx}}}\right)^2} \times 100. \tag{13}$$

As mentioned earlier, the development of WPT requires two resonators, one each working as Tx and Rx, which

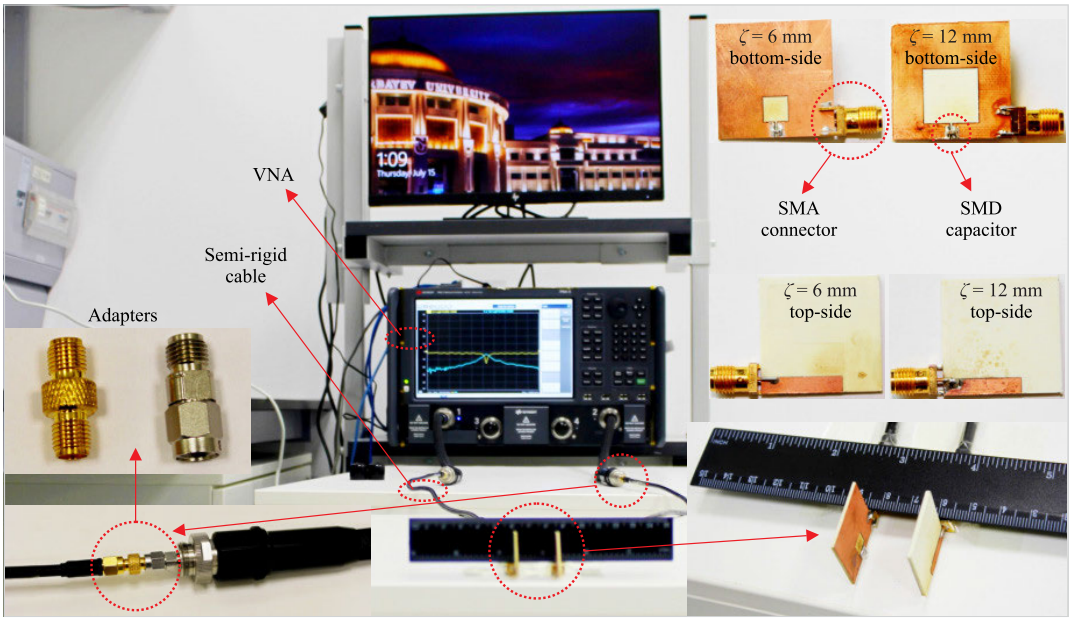

FIGURE 10. WPT measurement setup and fabricated resonator prototypes.

TABLE 3. Parameters of fabricated resonators for WPTs.

	C_e (pF)	α (mm)	γ (mm)
$\zeta = 6$ mm	3	16.7	3.4
$\zeta = 12$ mm	0.9	16.4	3.4

are appropriately designed to meet the WPT specifications. Once these are brought in close proximity, the wireless power transfer starts. However, as a first step, from these coupled resonators working as the sub-optimal WPT, some key parameters must be extracted. This enables impedance matching between the resonators and 50-Ω ports P1/P2. This ensures that there are minimal losses at the ports. In this paper, the J-inverter technique was employed to match `Tx` and `Rx` to the 50-Ω ports whose details can be found in [23].

It has been demonstrated that changing the slot area has a more significant impact than altering the shape. Therefore, the square slot-based resonator with two different slot areas (*i.e.*, $\zeta = 6$ mm and $\zeta = 12$ mm) were selected to show the influence of this new finding on the WPT system performance. The resonator parameters for the WPT development are given in Table 3. The Rogers RO4350B substrate, with a permittivity of 3.48, was used for prototypes of the designed resonators. To develop the WPT systems, two identical resonators were fabricated, for both cases, and the SMD (surface-mount) capacitors were incorporated. It is worth noting that both realized WPTs work at the same frequency of 900 MHz. During the experimental test, it was ensured that the fabricated resonators of WPTs were coupled at 25 mm. Furthermore, Fig. 10 depicts the general WPT measurement setup and realized two WPTs. Moreover, SMA (sub-miniature version A) connectors were employed in order to connect transmitting and receiving resonators to the semi-rigid cables. In turn, they were connected to the probes of employed VNA (PNA-X, N5247B) by means of two adapters. Consequently, this allows the measurement of $|S|$-parameters of WPTs, which can then be utilized to compute PTE employing (14) [19].

$$PTE = \frac{|S_{21}|^2}{1 - |S_{11}|^2}. \tag{14}$$

The simulation and measurement results, depicted in Fig. 11, show a very good agreement for both example prototypes. The values of $|S_{11}|$ convey that these resonators used in the development of WPT possess remarkable impedance matching at the chosen frequency. On the other hand, the values of $|S_{21}|$ demonstrate an excellent transmission capability at the operating frequency of 900 MHz. These outcomes can be used to calculate PTE of the developed WPTs using (14). The respective simulated efficiencies obtained from EM simulation results for ζ of 6 mm and 12 mm are 78% and 72%. The corresponding experimental values for ζ of 6 mm and 12 mm are 73% and 62%, accordingly. It is clear from both simulation and experimental results that PTE for WPTs with smaller ζ is higher when compared to PTE for WPTs having bigger ζ. Furthermore, there was a 6% decline in PTE during the simulation whereas the reduction in the experimental value was 11% for the two example cases. *This outcome once more highlights the extreme importance of Q in the practical realization of high-performance WPT systems*. Just to reiterate, the larger slots (signified by greater ζ) lead to lower Q. On a side note, PTEs degrade more during the experiments, as compared to the simulations, owing to the non-idealities associated with all the used components and, thus, incur extra losses which ultimately lead to reduced PTE.

A few examples of recent SGP-type WPT systems are evaluated in Table 4 based on the performed analysis and

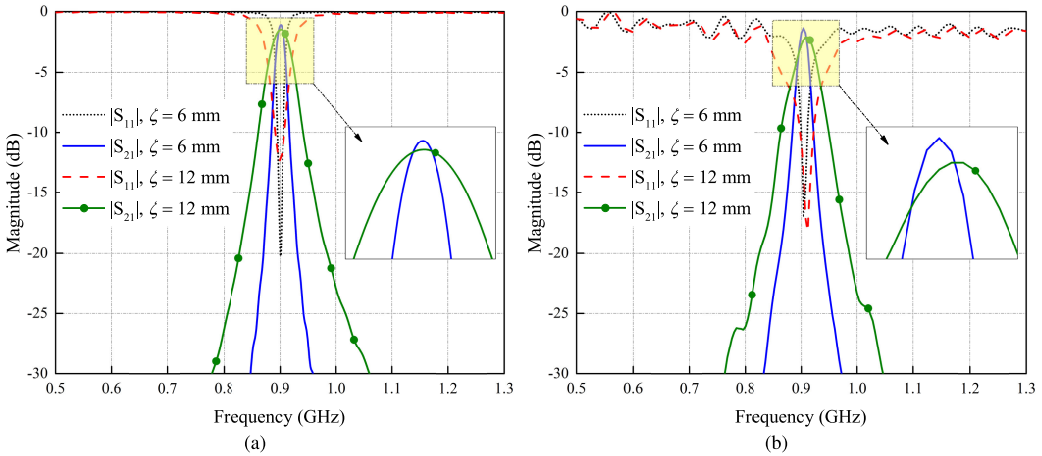

FIGURE 11. Obtained results of two developed WPTs, $|S|$-parameters vs frequency: (a) EM simulated; (b) experimental.

TABLE 4. The comparison with other SGP-based single- and multi-band WPT systems.

Ref.	Slot Type	Performed Analysis				Res-r Area mm × mm	f_0 (MHz)	PTD (mm)	PTE (%)	FoM
		SWF	H-field	RL	Q					
[10]	Elliptic Coils	–	–	–	–	30 × 15	49.6/149	15	71/66	0.36/0.33
[11]	Spiral	–	–	–	–	20 × 20	49	10	62	0.39
[12]	Squares	–	–	–	–	43 × 38	300/433/700	23	70.1/66/65	0.4/0.38/0.37
[13]	Spiral	–	–	–	–	20 × 20	190/1400	10	97/95	0.47/0.46
[17]	C-type	–	–	–	–	18 × 18	381/750	11	60/54	0.4/0.36
[18]	U	–	–	–	–	15 × 10	2400/5800	3.5	60/67	0.17/0.19
[23]	Polygon	✓	✓	–	–	25 × 25	900	25	62	0.62
This work	**Polygon**	–	–	✓	✓	25 × 25	900	25	73	0.73

the achieved experimental outcomes. Although the published works had decent results still it is noticeable that they overlooked analyzing the employed slot geometries in terms of the key parameters such as SWF, H-field, RL, and Q. Instead, authors primarily concentrated on the design challenges that heavily rely on the eventual WPT system specifications. The investigations and outcomes of this work, however, highlight the importance of a comprehensive analysis in developing high-performance WPT. In particular, the developed WPT system demonstrated the highest FoM value as compared to the other WPT systems.

V. CONCLUSION

Systematic analysis to understand the behavior of single-loop polygonal slot-based resonators has been reported in this paper. The emphasis has been on achievable Q and RL using various slots as these are the key parameters of resonators. It has been demonstrated that the area of the proposed slot plays a major role in resonator performance when compared to different shape types. The new findings, from the carried-out investigations and analysis, can facilitate the realization of high-performance yet robust WPT systems. Moreover, it has been reported that the WPTs utilizing such resonators can be designed in a first-pass manner with excellent agreement between the simulation and experimental results. In particular, it has been shown that the increase of 11% in PTE was achieved experimentally by WPT having a smaller slot area when two WPTs with different slot areas were compared.

REFERENCES

[1] N. Abbas, A. Basir, A. Iqbal, M. Yousaf, A. Akram, and H. Yoo, "Ultra-miniaturized antenna for deeply implanted biomedical devices," *IEEE Access*, vol. 10, pp. 54563–54571, 2022.

[2] H.-J. Kim, H. Hirayama, S. Kim, K. J. Han, R. Zhang, and J.-W. Choi, "Review of near-field wireless power and communication for biomedical applications," *IEEE Access*, vol. 5, pp. 21264–21285, 2017.

[3] S. A. A. Shah and H. Yoo, "Radiative near-field wireless power transfer to scalp-implantable biotelemetric device," *IEEE Trans. Microw. Theory Techn.*, vol. 68, no. 7, pp. 2944–2953, Jul. 2020.

[4] A. M. Mahmood, "Near-field wireless power transfer used in biomedical implants: A comprehensive review," *IET Power Electron.*, vol. 15, no. 16, pp. 1936–1955, Jul. 2022.

[5] K. Dautov, "Compact multi-frequency system design for SWIPT applications," *Int. J. RF Microw. Comput. Aided Eng.*, vol. 31, no. 6, Mar. 2021, Art. no. e22632.

[6] S. D. Barman, A. W. Reza, N. Kumar, M. E. Karim, and A. B. Munir, "Wireless powering by magnetic resonant coupling: Recent trends in wireless power transfer system and its applications," *Renew. Sustain. Energy Rev.*, vol. 51, pp. 1525–1552, Nov. 2015.

[7] R. Das, A. Basir, and H. Yoo, "A metamaterial-coupled wireless power transfer system based on cubic high-dielectric resonators," *IEEE Trans. Ind. Electron.*, vol. 66, no. 9, pp. 7397–7406, Sep. 2019.

[8] R. Chai and A. Mortazawi, "A position-insensitive wireless power transfer system employing coupled nonlinear resonators," *IEEE Trans. Microw. Theory Techn.*, vol. 69, no. 3, pp. 1752–1759, Mar. 2021.

[9] G. Monti, F. Mastri, M. Mongiardo, L. Corchia, and L. Tarricone, "Load-independent operative regime for an inductive resonant WPT link in parallel configuration," *IEEE Trans. Microw. Theory Techn.*, vol. 68, no. 5, pp. 1809–1818, May 2020.

[10] A. Barakat, S. Alshhawy, K. Yoshitomi, and R. K. Pokharel, "Simultaneous wireless power and information transfer using coupled co-existing defected ground structure resonators," *IEEE Trans. Circuits Syst. II, Exp. Briefs*, vol. 68, no. 2, pp. 632–636, Feb. 2021.

[11] S. Alshhawy, A. Barakat, K. Yoshitomi, and R. K. Pokharel, "Compact and efficient WPT system to embedded receiver in biological tissues using cooperative DGS resonators," *IEEE Trans. Circuits Syst. II, Exp. Briefs*, vol. 69, no. 3, pp. 869–873, Mar. 2022.

[12] S. Verma, D. Rano, S. Malhotra, and M. S. Hashmi, "Measurements and characterization of a newly developed novel miniature WIPT system," *IEEE Trans. Instrum. Meas.*, vol. 70, pp. 1–11, 2021.

[13] H. A. Atallah, R. Hussein, and A. B. Abdel-Rahman, "Tunable dual band wireless power transfer (TDB-WPT) system for short range applications," *IEEE Trans. Circuits Syst. II, Exp. Briefs*, vol. 70, no. 2, pp. 476–480, Feb. 2023.

[14] M. M. A. El Negm, H. A. Atallah, A. Allam, and A. B. A. El Rahman, "Design of compact coupled resonators for triple-band wireless power transfer," *IEEE Microw. Wireless Compon. Lett.*, vol. 31, no. 8, pp. 941–944, Aug. 2021.

[15] S. A. A. Shah, Y.-H. Lim, and H. Yoo, "A novel development of endovascular aortic stent system featuring promising antenna characteristics," *IEEE Trans. Antennas Propag.*, vol. 70, no. 3, pp. 2214–2222, Mar. 2022.

[16] D. Tang, C. Han, Z. Deng, H. J. Qian, and X. Luo, "Substrate-integrated defected ground structure for single- and dual-band bandpass filters with wide stopband and low radiation loss," *IEEE Trans. Microw. Theory Techn.*, vol. 69, no. 1, pp. 659–670, Jan. 2021.

[17] X. Jiang, F. Tahar, T. Miyamoto, A. Barakat, K. Yoshitomi, and R. K. Pokharel, "Efficient and compact dual-band wireless power transfer system through biological tissues using dual-reference DGS resonators," in *IEEE MTT-S Int. Microw. Symp. Dig.*, Jun. 2021, pp. 54–57.

[18] S. Verma, D. Rano, and M. Hashmi, "A novel dual band defected ground structure for short range wireless power transfer applications," in *Proc. IEEE Wireless Power Transf. Conf. (WPTC)*, Jun. 2019, pp. 188–191.

[19] K. Dautov, M. Hashmi, G. Nauryzbayev, and N. Nasimuddin, "Recent advancements in defected ground structure-based near-field wireless power transfer systems," *IEEE Access*, vol. 8, pp. 81298–81309, 2020.

[20] S. Y. Huang and Y. H. Lee, "A compact E-shaped patterned ground structure and its applications to tunable bandstop resonator," *IEEE Trans. Microw. Theory Techn.*, vol. 57, no. 3, pp. 657–666, Mar. 2009.

[21] Y. Rao, H. J. Qian, B. Yang, R. Gómez-García, and X. Luo, "Dual-band bandpass filter and filtering power divider with ultra-wide upper stopband using hybrid microstrip/DGS dual-resonance cells," *IEEE Access*, vol. 8, pp. 23624–23637, 2020.

[22] H. Liu, Z. Li, and X. Sun, "Compact defected ground structure in microstrip technology," *Elect. Lett.*, vol. 41, no. 3, pp. 1–2, Feb. 2005.

[23] K. Dautov, M. S. Hashmi, N. Nasimuddin, M. A. Chaudhary, and G. Nauryzbayev, "Quantifying the impact of slow wave factor on closed-loop defect-based WPT systems," *IEEE Trans. Instrum. Meas.*, vol. 71, pp. 1–10, 2022.

[24] K. Lee, C. Jeong, and S. Ho Chae, "Analysis of factors effecting on optimal configuration of two receivers for a three-coil wireless power transfer system," *IEEE Syst. J.*, vol. 13, no. 2, pp. 1328–1331, Jun. 2019.

[25] D. M. Pozar, *Microwave Engineering*, 4th ed. Hoboken, NJ, USA: Wiley, 2011, pp. 272–312.

[26] T. Sarkar, "DGS-integrated air-loaded wideband microstrip antenna for X- and Ku-band," *IEEE Antennas Wireless Propag. Lett.*, vol. 19, no. 1, pp. 114–118, Jan. 2020.

[27] C. Kumar and D. Guha, "Asymmetric and compact DGS configuration for circular patch with improved radiations," *IEEE Antennas Wireless Propag. Lett.*, vol. 19, no. 2, pp. 355–357, Feb. 2020.

[28] C. Caloz, H. Okabe, T. Iwai, and T. Itoh, "A simple and accurate model for microstrip structures with slotted ground plane," *IEEE Microw. Wireless Compon. Lett.*, vol. 14, no. 4, pp. 133–135, Apr. 2004.

[29] J.-S. Lim, S.-W. Lee, C.-S. Kim, J.-S. Park, D. Ahn, and S. Nam, "A 4.1 unequal Wilkinson power divider," *IEEE Microw. Wireless Compon. Lett.*, vol. 11, no. 3, pp. 124–126, Mar. 2001.

[30] D.-J. Woo, T.-K. Lee, and J. W. Lee, "Equivalent circuit model for a simple slot-shaped DGS microstrip line," *IEEE Microw. Wireless Compon. Lett.*, vol. 23, no. 9, pp. 447–449, Sep. 2013.

[31] C. Han, D. Tang, Z. Deng, H. Jenny Qian, and X. Luo, "Filtering power divider with ultrawide stopband and wideband low radiation loss using substrate integrated defected ground structure," *IEEE Microw. Wireless Compon. Lett.*, vol. 31, no. 2, pp. 113–116, Feb. 2021.

[32] C. Chen, X. Hou, and J. Wang, "A novel hybrid plasmonic resonator with high quality factor and large free spectral range," *IEEE Sensors J.*, vol. 21, no. 2, pp. 1644–1654, Jan. 2021.

[33] A. L. F. Stein, P. A. Kyaw, and C. R. Sullivan, "Wireless power transfer utilizing a high-Q self-resonant structure," *IEEE Trans. Power Electron.*, vol. 34, no. 7, pp. 6722–6735, Jul. 2019.

[34] J. Barreto, A.-S. Kaddour, and S. V. Georgakopoulos, "Conformal strongly coupled magnetic resonance systems with extended range," *IEEE Open J. Antennas Propag.*, vol. 1, pp. 264–271, 2020.

[35] D.-J. Woo, T.-K. Lee, J.-W. Lee, C.-S. Pyo, and W.-K. Choi, "Novel U-slot and V-slot DGSs for bandstop filter with improved Q factor," *IEEE Trans. Microw. Theory Techn.*, vol. 54, no. 6, pp. 2840–2847, Jun. 2006.

[36] T. H. Kim, "Asymmetric coil structures for highly eficient wireless power transfer systems," *IEEE Trans. Microw. Theory Techn.*, vol. 66, no. 7, pp. 3443–3451, Jul. 2018.

[37] T.-H. Kim, G.-H. Yun, W. Lee, and J.-G. Yook, "Highly efficient WPT system with negative impedance converter for Q-factor improvement," *IEEE Access*, vol. 7, pp. 108750–108760, 2019.

KASSEN DAUTOV received the B.Sc. degree (Hons.) in radio engineering, electronics, and telecommunications from Kazakh National Research Technical University (named after K. I. Satpayev), Almaty, Kazakhstan, in 2009, the M.Sc. degree in electronics engineering from the Bremen University of Applied Sciences, Bremen, Germany, in 2015, and the Ph.D. degree in science, engineering, and technology from Nazarbayev University, Astana, Kazakhstan, in 2023. He is currently a Postdoctoral Research Fellow with the School of Engineering and Digital Sciences, Nazarbayev University. His research interests include broad areas of antenna and high-frequency circuit design, with a particular focus on wireless power transfer systems, energy harvesting, metamaterials, and the antennas utilized in wireless body area networks.

GALYMZHAN NAURYZBAYEV (Senior Member, IEEE) received the B.Sc. and M.Sc. degrees (Hons.) in radio engineering, electronics, and telecommunications from the Almaty University of Power Engineering and Telecommunication, Almaty, Kazakhstan, in 2009 and 2011, respectively, and the Ph.D. degree in wireless communications from The University of Manchester, U.K., in 2016. From 2016 to 2018, he held several academic and research positions with Nazarbayev University, Kazakhstan, L. N. Gumilyov Eurasian National University, Kazakhstan, and Hamad Bin Khalifa University, Qatar. In 2019, he joined Nazarbayev University with the rank of an Assistant Professor. His research interests include wireless communication systems, with a particular focus on reconfigurable intelligent surface-enabled communications, multiuser MIMO systems, cognitive radio, signal processing, energy harvesting, visible light communications, NOMA, and interference mitigation. He served as a technical program committee member for numerous IEEE flagship conferences. He is a member of the National Research Council of the Republic of Kazakhstan.

MOHAMMAD HASHMI (Senior Member, IEEE) received the B.Tech. degree from Aligarh Muslim University, India, the M.S. degree from the Darmstadt University of Technology, Germany, and the Ph.D. degree from Cardiff University, Cardiff, U.K. He had held research, engineering, and academic positions with the University of Calgary, Canada; Cardiff University; Thales Electronics GmbH, Germany; Philips Technology Center, Germany; and IIIT Delhi, India. He is currently an Associate Professor with Nazarbayev University, Kazakhstan. His research activities have led to one book, three U.S. patents (two pending), and over 250 journals and conference publications. His current research interests include the domain of advanced RF circuits for wireless applications (including wireless power transfer and energy harvesting), emerging RF circuits and applications, broadband linear and efficient power amplifiers for mobile and satellite applications, and high- and low-frequency instrumentation. He is an Associate Editor of *IEEE Microwave Magazine*.